Influence of the impact parameter on element distributions in dissipative heavy-ion collisions

H. J. Wollersheim,* W. W. Wilcke, J. R. Birkelund, and J. R. Huizenga
Nuclear Structure Research Laboratory and Departments of Chemistry and Physics, University of Rochester, Rochester, New York 14627
(Received 31 August 1981)

The $^{209}Bi+^{136}Xe$ reaction at laboratory bombarding energies of 940, 1130, and 1422 MeV is interpreted on the basis of a phenomenological classical model and a diffusion model for damped collisions. Initial angular momenta, interaction times, and charge diffusion coefficients are deduced with the above models from experimental data reported previously. The bombarding energy dependence of the model parameters and the effect of deformation on the dinuclear system in the exit channel are discussed. An analytical relation is suggested between the variance σ_Z^2 of the element distribution and the ratio E/l_g, where E is the measured final total kinetic energy and l_g is the grazing orbital angular momentum. This semiempirical formula is applied to sixteen heavy-ion systems at bombarding energies well above the Coulomb barrier. In a plot of $\ln\sigma_Z^2$ versus E/l_g all the experimental data fall on parallel lines with displacements that are reasonably well correlated with E_0/l_g, where E_0 is the bombarding energy in the c.m. system. In a model-dependent explanation of this empirical relation, evidence is found that the variance of the element distributions σ_Z^2 is determined by the initial relative angular momentum l/l_g.

[NUCLEAR REACTIONS $^{209}Bi(^{136}Xe,HI)$, $E_{lab}=940$, 1130, and 1422 MeV; deduced initial angular momentum, interaction time and charge diffusion coefficient; strongly damped reaction; systematics of heavy-ion reaction data.]

I. INTRODUCTION

During the past few years, relaxation phenomena in heavy-ion collisions have been an interesting subject of experimental and theoretical studies. Among the various observables that are measured in damped collision, the amounts of dissipated kinetic energy and the widths of the final mass or element distributions are of special interest. In dissipative collisions, the observed element distributions of the light reaction fragment are generally centered close to the charge (Z) of the projectile. For given energy losses, the distributions are nearly Gaussians, and their variances σ_Z^2 increase monotonically with the dissipated kinetic energy $E_{loss}(\equiv -Q$ value). The strong correlation between E_{loss} and σ_Z^2 was first pointed out by Huizenga *et al.*[1] Similar correlations were found for several systems in the mass region between $^{165}Ho+^{84}Kr$ and $^{209}Bi+^{136}Xe$. In further investigations, the importance of the total kinetic energy loss as a relevant parameter in the analysis of element distributions was confirmed, but it became apparent that the relation between the negative Q value and σ_Z^2 depends on the projectile-target combination (see, e.g., Fig. 11 of Ref. 2) and the available energy above the Coulomb barrier in the entrance channel, i.e., $E_0-V_C(R_{int})$ (see, e.g., Fig. 8 of Ref. 3).

In the present paper, the final element distributions are interpreted using a phenomenological model for the relative motion of the heavy ion. Uncertainties associated with classical trajectory calculations, due to specific assumptions about nuclear interaction potentials, friction coefficients, and shape of the intermediate system are largely avoided in a phenomenological model,[4-6] which relates the observed relaxation processes to a few model parameters. As a result of the analysis, a new systematics of the experimental data is found, which is remarkable due to the fact that for different projectile-target combinations and bombarding energies, the variances of the element distribution depend in a unique way on the final total kinetic energy and the grazing angular momentum.

It is shown that in the framework of the model, the observed correlation can be traced back to a dependence of σ_Z^2 on the impact parameter ratio b/b_g. Since mass distribution data are still relatively scarce, the present investigation is confined to element distributions, although a similar analysis is expected to apply to the more fundamental mass distributions.

Detailed calculations are carried out for the ^{209}Bi+^{136}Xe reactions at E_L=940, 1130, and 1422 MeV.[3,7,8] The results of these analyses are representative of damped collisions and follow the systematics of other available experimental data. In Sec. II, the common features of sixteen heavy-ion systems are demonstrated. The analysis of damped heavy-ion reactions based on a phenomenological model for the relative motion and on a diffusion model[9] is described in Sec. III. For the ^{209}Bi+^{136}Xe reaction at three bombarding energies, the deduced model parameters, including the initial angular momenta, nuclear interaction times, and charge diffusion coefficients, are presented and discussed. All results are combined in Sec. IV to yield a unique correlation between the variance of the Z distribution and the initial relative angular momentum l/l_g. A summary is given in Sec. V.

II. EMPIRICAL CORRELATION OF EXPERIMENTAL OBSERVABLES FOR DAMPED HEAVY-ION REACTIONS

This section presents a new empirical correlation between experimental observables measured in the characterization of damped heavy-ion reactions. This correlation describes the dependence of the variance σ_Z^2 of the element distribution on the ratio, E/l_g, of the final total kinetic energy E and the grazing angular momentum l_g. Results on sixteen heavy-ion systems (Refs. 1, 3, 4, 8, and 10–17) ($221 \leq A_P + A_T \leq 476$) at bombarding energies well above the Coulomb barrier [$E_0/V_C(R_{\text{int}}) \geq 1.2$] are discussed in the new representation of $\ln\sigma_Z^2$ vs E/l_g. A heavy-ion system is defined here as a particular target-projectile combination interacting with a specified initial center-of-mass energy E_0. One of the interesting features of this relation is that the experimental data are seen to define approximately parallel lines of $\ln\sigma_Z^2$ vs E/l_g for different heavy-ion systems. This finding is displayed in Fig. 1, where $\ln\sigma_Z^2$ is plotted as a function of $(E/l_g)+C(X)$. Here $C(X)$ denotes a system-dependent constant chosen to shift the abscissa of each system X in order to demonstrate the unique slope of the semilogarithmic function. Figure 1 contains 127 data points from the sixteen heavy-ion systems listed in the figure. These reactions exhibit all types of angular distributions including orbiting, sharply focused, and Coulomb-like distributions. The grazing angular momentum for each system is determined either from the quarter-point angle [see Eq. (3.3)] or, if elastic scattering data are not available, from systematic studies[18] of the interaction radius R_{int}. The residual spread of the points in Fig. 1 about a common slope may be partially due to variations in data analyses. For example, some of the Z distributions

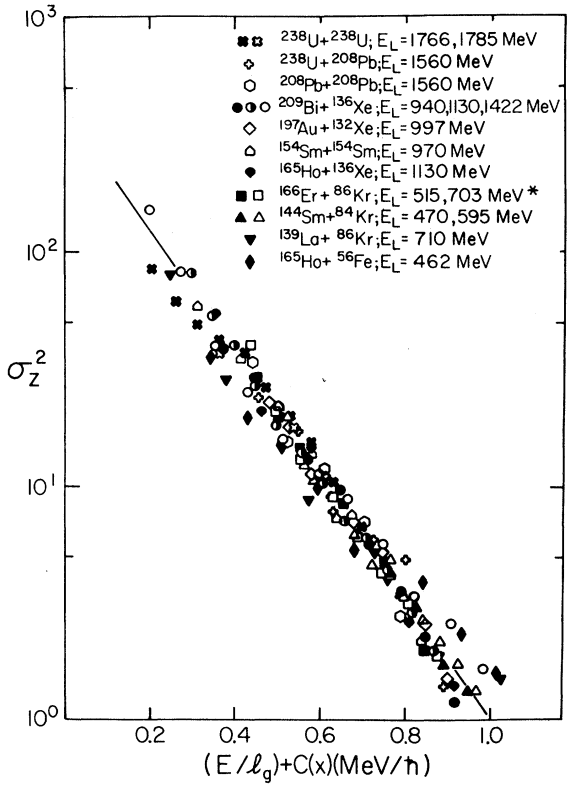

FIG. 1. Dependence of the variance of the element distribution σ_Z^2 on the ratio E/l_g for various projectile-target combinations, where E is the final total kinetic energy and l_g is the grazing angular momentum. A system-dependent contant $C(X)$ is added to E/l_g in order to demonstrate the universal slope of the correlation. The experimental data are from Refs. 1, 3, 7, 8, and 10–17. The reaction where the σ_Z^2 data are determined for energy bins corrected for different Coulomb potentials in the entrance and exit channels is marked with an asterisk.

are analyzed for energy bins corrected for different Coulomb potentials in the entrance and exit channels (reaction marked with an asterisk in Fig. 1), while other Z distributions are grouped as a function of Q value. Furthermore, some of the earliest data were not corrected for neutron evaporation in the evaluation of the Q value. Typical error bars for the variance of the element distribution are 10—20 %, depending on the Q value.

The solid line in Fig. 1 represents the result of a least-squares fit to all the data yielding a value for the slope of -6.07 ($\hbar$/MeV). This average slope is subsequently used to determine the displacement $C(X)$ of the individual parallel lines from the common line of Fig. 1 when the experimental data of $\ln\sigma_Z{}^2$ are plotted against E/l_g. Each value of $C(X)$ is obtained from a fit to the data of the corresponding system, according to the linear function,

$$\ln\sigma_Z{}^2 = -6.07[(E/l_g) + C(X) - 1] , \tag{2.1}$$

where $(E/l_g)+C(X)=1$ when $\ln\sigma_Z{}^2=0$ ($\sigma_Z{}^2=1$). The range of applicability of Eq. (2.1) is limited to $\sigma_Z{}^2$ values approximately equal to or greater than one. In Fig. 2 the resulting value of $1-C(X)$ for each of sixteen heavy-ion systems is plotted as a function of the corresponding ratio E_0/l_g, where E_0 is the initial center-of-mass energy and l_g is the grazing angular momentum. The choice of the abscissa in Fig. 2 is motivated by the fact that $\ln\sigma_Z{}^2=0$ is associated with very small energy losses where the kinetic energy is approaching the incident energy E_0. Hence, the curves of $\ln\sigma_Z{}^2$ vs E/l_g will all cross the abscissa defined at $\ln\sigma_Z{}^2=0$ at values of E/l_g approximately equal to E_0/l_g. Thus, the values of $1-C(X)$ which define the intercept (at $\ln\sigma_Z{}^2=0$) on the abscissa in Eq. (2.1) are approximately equal to E_0/l_g. This accounts for the strong correlation observed in Fig. 2. The dashed line in Fig. 2 is the result of a linear function fitted to the plotted points and corresponds to

$$1-C(X)=1.393E_0/l_g-0.651 . \tag{2.2}$$

A typical uncertainty of 6% in a particular value results, if one uses Eq. (2.2) for calculating the constant $1-C(X)$. It should be noted, however, that with the availability of additional heavy-ion data the numerical values of the average slope and the related $[1-C(X)]$ parameters may change slightly. At present, Eq. (2.2) can be substituted into Eq. (2.1) to evaluate the dependence of $\sigma_Z{}^2$ on the ratio E/l_g. This relationship may be used to predict experimental results for different

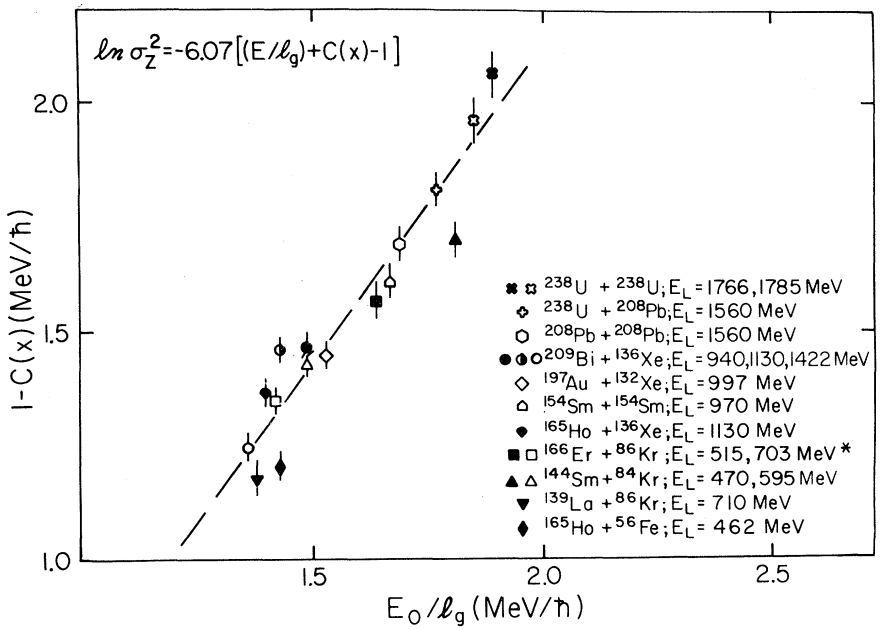

FIG. 2. Correlation between $[1-C(X)]$ values and the ratio E_0/l_g of the bombarding energy E_0 in the c.m. system to the grazing angular momentum l_g. The dashed line represents the result of a linear function fitted to the experimental data.

projectile-target combinations and higher incident energies. For an extrapolation to higher bombarding energies, it is important to realize that the quantity E_0/l_g does not continue to decrease monotonically with increasing values of E_0 but has a minimum value for each projectile-target combination. For incident energies larger than 2 $V_C(R_{\rm int})$, the ratio E_0/l_g increases again into the region where Eq. (2.2) is well established by the heavy-ion reactions investigated. An example of a heavy-ion system where E_0 exceeds 2 $V_C(R_{\rm int})$ is the ^{166}Er+^{86}Kr reaction measured[19] recently at 12.1 MeV/nucleon, where $E_0/l_g=1.46$ MeV/$\hbar$. The semilogarithmic plot of the average $\sigma_Z{}^2$ values versus E/l_g confirms the unique slope shown in Fig. 1 and yields a $[1-C(X)]$ parameter of 1.38 MeV/$\hbar$, a value which is in agreement with the systematic trend shown in Fig. 2.

As shown in Fig. 1, a large collection of heavy-ion reaction data are systematically correlated by the simple relationship given in Eq. (2.1). In the following sections the ^{209}Bi+^{136}Xe reaction, measured at three quite different bombarding energies, will be analyzed with a phenomenological reaction model to search for the underlying fundamental reaction features responsible for the observed systematics.

III. PHENOMENOLOGICAL ANALYSIS OF STRONGLY DAMPED COLLISIONS

A. Outline of the phenomenological model

The relationship between the variance $\sigma_Z{}^2$ of the element distribution and E/l_g for damped heavy-ion reactions, shown in Fig. 1, will be made plausible in this and subsequent sections by consideration of several model-dependent quantities. In this section a brief outline of the general model is given in order to guide the reader through the subsequent sections.

In a simple diffusion model,[9] the variance of the Z distribution, $\sigma_Z{}^2$, increases linearly with the nuclear interaction time, $t_{\rm int}$, according to

$$\sigma_Z{}^2=2D_Z t_{\rm int}\ , \tag{3.1}$$

where D_Z denotes a constant average charge diffusion coefficient and $t_{\rm int}$ is the time interval between the formation and rupture of the dinuclear system. The mean interaction time is determined by the impact parameter b or the corresponding initial angular momentum l, if a classical scattering picture is assumed. For grazing collisions ($l=l_g$) the interaction time is very small, because there is little nuclear interaction between projectile and target nuclei. With decreasing values of l, the nuclear interaction time increases and, as shown previously,[20-21] $t_{\rm int}$ may be represented by an exponential function of the initial relative angular momentum l/l_g. If this approximation of the interaction time is substituted into Eq. (3.1), the functional form of the resulting expression suggests a plot of $\ln\sigma_Z{}^2$ vs l/l_g. Figure 1 is such a plot where, however, the model parameter l is replaced by the measured final total kinetic energy E. This replacement is plausible based on a reported[7,8,22] nearly linear relationship between $\langle l\rangle$ and $\langle E\rangle$.

The following subsections will present a detailed analysis of the ^{209}Bi+^{136}Xe reaction at $E_L=940$, 1130, and 1422 MeV and discuss various correlations of the final total kinetic energy, nuclear interaction time, and charge diffusion coefficient as a function of the initial angular momentum.

B. Mean initial angular momentum

For strongly damped heavy-ion reactions the wave length $\lambda\!\!\!^{-}$ of the relative motion is much smaller than the characteristic length $R_{\rm int}$ of the nuclear interaction potential between the two nuclei. Hence, for such reactions, it is meaningful to utilize the concept of a classical trajectory determined by the impact parameter. Outside the range of nuclear interaction, the relative motion is completely determined by the electromagnetic interaction alone. For large angular momenta, these trajectories follow approximately Coulomb orbits. At angular momenta smaller than the grazing angular momentum l_g, nuclear reactions become significant and the "elastic" cross section, which is defined to contain also the cross section of the Coulomb-excited states, falls off sharply with decreasing impact parameter. This rapid transition from Coulomb scattering to nuclear absorption within a narrow and well-defined region of separation distances close to $R_{\rm int}$ leads to simple formulas for the "elastic" scattering and total reaction cross sections, which are essentially of a geometrical nature and independent of the details of nuclear structure. In the generalized Fresnel model of Frahn,[23] the total reaction cross section is given by

$$\sigma_R=\pi k_\infty{}^{-2}\left[\left(l_g+\tfrac{1}{2}\right)^2+2\delta\left(l_g+\tfrac{1}{2}\right)+\left(\pi^2/3\right)\delta^2\right], \tag{3.2}$$

where

$$l_g = \eta \cot\left[\tfrac{1}{2}\theta_{1/4}\right] . \tag{3.3}$$

The quantities k_∞, η, and $\theta_{1/4}$ denote the asymptotic wave number, the Coulomb parameter, and the quarter-point angle in the center-of-mass system. The value of the l-space "window" parameter δ is determined from the slope of $\ln(d\sigma_{\text{elastic}}/d\sigma_{\text{Rutherford}})$.

For decreasing angular momentum $l < l_g$, the scattering angle does not continue to increase as in a pure Coulomb interaction. The nuclei are affected by the attractive nuclear potential such that trajectories may be deflected forward or focused near the quarter-point angle as, for example, observed for the ^{209}Bi+^{136}Xe collisions.[3,7,8] Very instructive for a classification of the measured angular distributions are contour plots of $d^2\sigma/dE\,d\Omega_{\text{c.m.}}$ as a function of the center-of-mass angle θ and the final total kinetic energy E (Wilczyński plot). These plots show the evolution of the mean deflection angle $\theta(E)$ from the elastic to the fully relaxed events. The gross structure depends strongly on the relative magnitude of the attractive nuclear force and the repulsive Coulomb and centrifugal forces. The balance between these forces can be varied by changing either the bombarding energy or the charge product $Z_P Z_T$ of the projectile and target nuclei.

The systematic patterns that are evident from the overall dependence of the cross section on angle, energy, and charge partition in the exit channel may arise from characteristic reaction variables such as the initial angular momentum or nuclear interaction time. Although these quantities are not directly observable, they play a central role in the theoretical interpretation of the data. In this and following sections, the experimental results of the ^{209}Bi+^{136}Xe reaction are related to these and other model-dependent quantities. In performing such analyses, the above reaction has the advantage that the probability for compound-nucleus formation is negligible and, hence, the difficulty of separating the two superimposed reaction types, damped and fusion reactions, is minimized.

For the determination of mean initial angular momentum, a procedure is used that was first proposed by Schröder *et al.*[6] The basic assumption of this procedure relates to a monotonic increase in the excitation energy (i.e., the negative Q value) of the two nuclei with decreasing values of the initial angular momentum l. Using the generalized Fresnel model [Eq. (3.2)] and the experimental differential cross section as a function of energy loss, a mean initial angular momentum is related to a mean final total kinetic energy according to

$$\Delta\sigma_{n,n-1} = \pi k_\infty^{-2}\left[\left[l_n+\tfrac{1}{2}\right]^2 - \left[l_{n-1}+\tfrac{1}{2}\right]^2 + 2\delta\left[l_n - l_{n-1}\right]\right] , \tag{3.4}$$

where $\Delta\sigma_{n,n-1}$ is the damped reaction cross section measured in an energy window between E_n and E_{n-1}. Starting with a zero Q value and the corresponding angular momentum l_g, an average initial angular momentum is determined for each energy bin by a successive procedure illustrated previously.[21] This type of analysis is applied to the ^{209}Bi+^{136}Xe reaction at $E_L = 1422$ MeV[3] with the model parameters $l_g = 63\hbar$ and $\delta = 8\hbar$ obtained from the elastic scattering data. The results are presented in Fig. 3 together with values of two earlier measurements[7,8] at $E_L = 940$ and 1130 MeV.

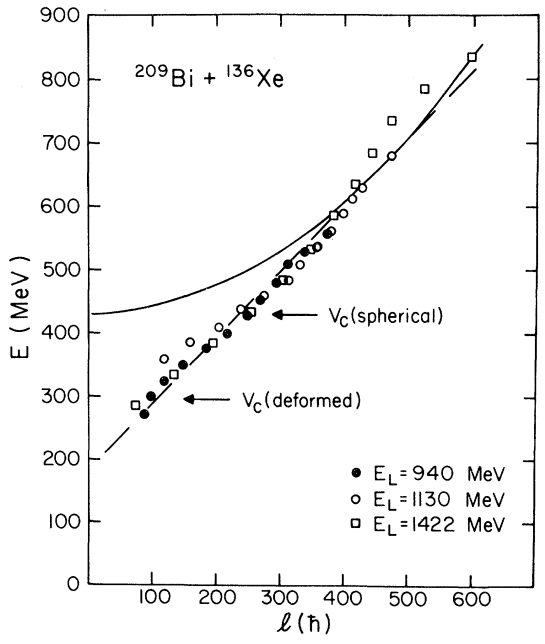

FIG. 3. The mean final kinetic energy E is plotted versus the mean initial angular momentum l for the ^{209}Bi+^{136}Xe reaction at $E_L = 940$, 1130, and 1442 MeV. The dashed line is a least-squares fit to the data. The solid curve represents the energy-angular momentum relation for grazing collisions [Eq. (3.6)]. The arrows indicate the Coulomb potential in the entrance channel, i.e., V_C (spherical) and the limiting Coulomb potential in the exit channel, i.e., V_C (deformed).

A nearly linear relationship exists between $\langle E \rangle$ and $\langle l \rangle$ independent of the bombarding energy (see Fig. 3). Thus, for the ^{209}Bi+^{136}Xe reaction at three bombarding energies, the final total kinetic energy is parametrized as

$$\langle E \rangle = (183.7 \pm 9.2) + (1.055 \pm 0.029)\langle l \rangle \ , \tag{3.5}$$

where $\langle E \rangle$ is given in MeV and l in units of $\hbar$. The dashed line in Fig. 3 is calculated with Eq. (3.5). The solid curve in Fig. 3 depicts the energy-angular momentum relation for grazing collisions ($l = l_g$), given by

$$E(l) = \frac{Z_P Z_T e^2}{R_{\text{int}}} + \frac{\hbar^2 l^2}{2\mu R_{\text{int}}^2} \tag{3.6}$$

and determines the starting point for all possible ^{209}Bi+^{136}Xe reactions. Alternatively, it describes the dependence of the final total kinetic energy on the initial angular momentum, if one assumes that the radial kinetic energy of the system is dissipated at the interaction radius R_{int} and that the angular momentum is preserved. Since the identities of the two reacting nuclei are preserved to a large extent during the collision process, the charge numbers (Z_P,Z_T) and mass numbers (A_P,A_T) of the final fragments may be replaced by those of the projectile and target nuclei. A constant interaction radius R_{int} of 15 fm is derived from the experimental quarter-point angles measured for the ^{209}Bi+^{136}Xe reaction in a bombarding-energy range of 1.9 to 5.3 MeV/nucleon above the Coulomb barrier V_C (spherical) in the entrance channel. The effect of angular momentum dissipation during the collision on the calculated final total kinetic energy is estimated to be less than 10% based on the functional dependence of the gamma-ray multiplicity on the initial angular momentum as found for the ^{166}Er+^{86}Kr reaction.[24] As can be seen from Fig. 3, the correlation between $\langle E \rangle$ and $\langle l \rangle$ is reasonably well reproduced by Eq. (3.6) for mean initial angular momenta larger than 400$\hbar$. Based on this result, one could conclude that for large l values the energy in radial motion is completely relaxed very quickly during the initial stage of the collision. If this were true, the dinuclear system ruptures at the interaction radius R_{int} and the assumption of "frozen" spherical fragment shapes may be a reasonable approximation for calculating the trajectories in the exit channel. However, on the other hand, the existence of a stretched configuration not be excluded for this region of l values. In this case the Coulomb energy and centrifugal energy in the exit channel are both reduced and this energy deficit is compensated by a radial kinetic energy in order to give the observed final total kinetic energy.

For mean initial angular momenta smaller than 400$\hbar$, the increasing deviation of the points in Fig. 3 from the solid curve given by Eq. (3.6) with decreasing l is evidence for a deformed dinuclear system at scission. The maximum elongation observed is independent of the bombarding energy for the ^{209}Bi+^{136}Xe reaction and agrees with predictions for a normal fission process. Using the empirical formula of Viola,[25] modified slightly for asymmetric fission,[18] a minimum kinetic energy of 295 MeV is calculated for the ^{209}Bi+^{136}Xe systems, in good agreement with the measured value of 270±30 MeV. Three points on the correlation plot of $\langle E \rangle$ vs $\langle l \rangle$, shown in Fig. 3, result directly from the Fresnel model[23] at the values of E_0 and the corresponding value of l_g for the three experiments studied. With increasing bombarding energy, the range of initial angular momenta extends to larger l values and, hence, the fraction of the damped reaction cross section known to proceed through stretched scission shapes is less important.

The relationship between the measured final total kinetic energy and the deduced mean initial angular momentum is illustrated also in Fig. 4. The sum of the Coulomb and centrifugal potentials is plotted as a function of the distance r between the centers of the fragments. For the ^{209}Bi+^{136}Xe reaction at two bombarding energies, $E_0 = 569$ MeV ($E_L = 940$ MeV) and 861 MeV ($E_L = 1422$ MeV), dissipated energies of 250 MeV, for example, correspond to mean initial angular momenta of $\langle l \rangle = 128$ and 405$\hbar$, respectively. The interaction radius of $R_{\text{int}} \approx 15$ fm at which nuclear reaction is initiated in the entrance channel is indicated in Fig. 4. Based on such a plot, it is not possible to conclude that the fragments on the $l = 405\hbar$ trajectory separate at a scission distance larger than R_{int}. However, for the lower bombarding energy ($l = 128\hbar$), if for example, 250 MeV of energy is dissipated, the final total kinetic energy is 319 MeV ($V_C + V_{l=128\hbar}$), necessarily giving a highly deformed scission distance of about 21.5 fm. If one assumes angular momentum dissipation ($l_f < l$), the scission distance is decreased by less than 0.5 fm because the Coulomb potential, represented by the dashed curve, is the dominant term in V_C

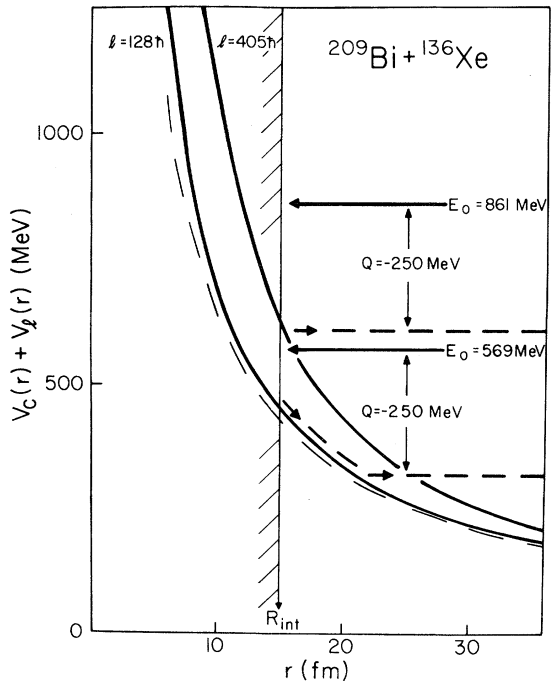

FIG. 4. Schematic representation of the combined Coulomb potential V_C and centrifugal potential V_l for the ^{209}Bi+^{136}Xe reaction at two bombarding energies. An energy dissipation of 250 MeV corresponds to an initial angular momentum of $l=128$ and 405 $\hbar$ in the two cases. The dashed curve represents the Coulomb potential alone. The interaction radius $R_{\rm int}$ indicates the distance of closest approach for a grazing trajectory. From the measured final total kinetic energy no deformation of the fragments can be inferred for $E_0=861$ MeV ($E_L=1422$ MeV), while a stretched configuration of the composite system has to develop for $E_0=569$ MeV ($E_L=940$ MeV).

$+V_{l=128\hbar}$. On the basis of Figs. 3 and 4 it is obvious that damped reactions proceed with some probability through stretched dinuclear shapes in the exit channel. This is especially true when the bombarding energy is near the Coulomb barrier, because then nearly all impact parameters must lead to an elongated scission configuration.

C. Nuclear interaction time

From the maxima or centroids of the angular distribution for each energy bin $\langle E\rangle$ the experimental deflection function $\theta(l)$ can be constructed using the deduced correlation between the final total kinetic energy $\langle E\rangle$ and the initial angular momentum $\langle l\rangle$. The resulting deflection function is often used to test theoretical scattering models. Instead of searching for an unique set of values of the nuclear interaction potential and the friction coefficient, the experimental results are related to an effective interaction time which characterizes the observed relaxation process. The deduced nuclear interaction time plays a central role in the transport model[9] which is discussed in part D of this section.

In the phenomenlogical treatment of the strongly damped reaction the projectile is assumed to approach the target nucleus on a Coulomb trajectory and starts to interact at the interaction radius through nuclear forces. A composite system of two interacting nuclei is formed which rotates about its center of mass. As long as the two nuclei are in close contact, mass is transferred and kinetic energy and angular momentum are dissipated. At a later stage of the collision the dinuclear system separates at the scission distance and the fragments move again on Coulomb trajectories. The time interval between formation and separation of the composite system is defined as the nuclear interaction time.

A method used to calculate the interaction time was introduced by Huizenga *et al.*[4,5,21] For a given initial angular momentum the interaction time $t_{\rm int}$ is defined by the rotation of the composite system

$$t_{\rm int}=\frac{\mathscr{I}[\theta_C(l)-\theta(l)]}{l\hbar}\ , \tag{3.7}$$

where

$$\mathscr{I}=\mu R_{\rm int}{}^2\ . \tag{3.8}$$

The quantities μ, $\theta(l)$, and $\mathscr{I}$ denote the reduced mass of the system, the experimental deflection function, and the relative moment of inertia at close contact. The Coulomb deflection function $\theta_C(l)$ is composed of contributions from the initial (i) and final (f) channels according to

$$\theta_C(l)=\pi-\theta_i-\theta_f\ , \tag{3.9}$$

where

$$\theta_i=\arccos\left[\frac{\eta_i{}^2}{\eta_i{}^2+l^2}\right]^{1/2} -\arccos\frac{l^2+\eta_i k_\infty R_{\rm int}}{k_\infty R_{\rm int}\left[\eta_i{}^2+l^2\right]^{1/2}} \tag{3.10a}$$

and

$$\theta_f = \arccos\left[\frac{\eta_f^2}{\eta_f^2 + l_f^2}\right]^{1/2} . \tag{3.10b}$$

Here k_∞ and l_f denote the asymptotic wave number in the entrance channel and the angular momentum in the exit channel, respectively. The Coulomb parameters are given by

$$\eta_{i,f} = \frac{Z_P Z_T e^2}{\hbar}\left(\frac{\mu}{2}\right)^{1/2}\begin{Bmatrix} E_0^{-1/2} & \text{initial channel} \\ E^{-1/2} & \text{exit channel} \end{Bmatrix} . \tag{3.11}$$

Note, that no second term appears in Eq. (3.10b) because the final total kinetic energy E can be written as

$$E = \frac{Z_P Z_T e^2}{R} + \frac{\hbar^2 l_f^2}{2\mu R^2} \tag{3.12}$$

if it is assumed that the radial part of the kinetic energy is completely dissipated when the system reaches the scission radius R.

The remaining parameter required to calculate an effective interaction time is the final angular momentum l_f which depends on the angular momentum transfer from relative to intrinsic motion. In the analysis presented here, two extreme cases are considered, (i) no angular momentum transfer, $l_f = l$ (nonsticking limit NS), and (ii) a reduction of the initial angular momentum to

$$l_f = (\mathcal{I}/\mathcal{I}_S) l , \tag{3.13}$$

(sticking limit S) where $\mathcal{I}_S = \mathcal{I} + \frac{2}{5}(M_P R_P^2 + M_T R_T^2)$ and M_P, M_T, R_P, and R_T are the mass and radius of projectile and target nucleus, respectively.

It should be noted here that a main object of the calculations is to find an approximate analytical expression for the interaction time as a function of impact parameter which can be applied to both limiting cases. The results for the interaction times are displayed in Fig. 5 as a function of the initial relative angular momentum l/l_g for the ^{209}Bi + ^{136}Xe reaction at $E_L = 940$, 1130, and 1422 MeV. In this representation the interaction time $t_{\text{int}}(l/l_g)$ is approximately independent of the bombarding energy. This interesting result has been obtained also for the ^{166}Er + ^{86}Kr reaction[20] at $E_L = 515$ and 703 MeV. Apart from the vicinity of the grazing angular momentum, the interaction time increases exponentially with decreasing l for both assumptions of angular momentum transfer. Therefore, t_{int} is approximated by the following

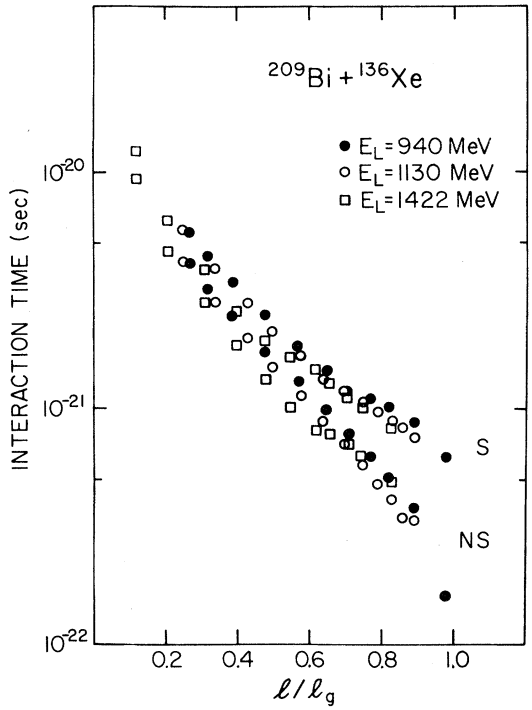

FIG. 5. The mean interaction time t_{int} is plotted as a function of the initial relative angular momentum l/l_g for the ^{209}Bi + ^{136}Xe reaction at $E_L = 940$, 1130, and 1422 MeV. The final angular momentum is calculated in the limits of the "nonsticking" NS and "sticking" S models.

analytical expression:

$$t_{\text{int}} = a \exp(-b l/l_g) , \tag{3.14}$$

where the constant a and b depend on whether the "nonsticking" or "sticking" model is used. In addition to the ^{209}Bi + ^{136}Xe reaction, the exponential dependence of the interaction time on the initial relative angular momentum is also obtained from the analysis of several other heavy-ion collisions (Refs. 17, 20–22, and 26–28).

D. Charge diffusion coefficient

The mean interaction times obtained in the previous section are used to calculate transport coefficients in a simple diffusion model.[9] This model emphasizes the statistical aspect of strongly damped heavy-ion reactions, where nucleons are transferred between the nuclei of the composite system in both directions. One application of a diffusion model to nuclear collisions is a study of the element distribution which broadens as the interaction time increases. According to Eq. (3.1)

the variance σ_Z^2 of the Z distribution is a linear function of the interaction time. From these two quantities the charge diffusion coefficient D_Z is deduced, where D_Z is defined in terms of a time-average value over the whole trajectory for a given impact parameter.

In order to determine the transport coefficients D_Z, one must employ l-dependent σ_Z^2 values. A relationship between the experimental total kinetic energy loss or negative Q value and the variance σ_Z^2 of the element distribution for the ^{209}Bi+^{136}Xe reaction at $E_L=940$, 1130, and 1442 MeV has been reported previously.[3,7,8] Accepting the results of Sec. III B as a valid description of the correlation between the final kinetic energy, $E=E_0+Q$, and the initial angular momentum l, one can immediately calculate the charge diffusion coefficient. Assuming the sticking model for the derivation of the interaction times, values of D_Z are calculated as a function of the initial relative angular momentum l/l_g. These results are shown in Fig. 6. For the three bombarding energies the charge diffusion coefficients are rather constant over a range of l values. However, for l values close to the grazing angular momentum l_g the transport coefficient D_Z decreases with increasing values of the initial relative angular momentum. The error bars shown for the charge diffusion coefficients include the uncertainties of the σ_Z^2 values, and as a limit for the interaction times, the assumption that the composite system starts to rotate at the distance of closest approach instead of the interaction radius R_{int}. At the interaction radius the density overlap between the two nuclei is only 5–10% of the central density and it seems to be rather unlikely that the sticking condition is fulfilled. The largest error, which is not included in Fig. 6, is caused by systematic uncertainties in separating the intensity of the elastic scattering from the damped cross section and hence, by the determination of the initial angular momentum. Although these deviations are small compared to the values displayed in Fig. 3, the interaction times are strongly affected due to the exponential dependence on l. The resulting additional relative systematic error of the charge diffusion coefficient can be as large as 50%. For the three ^{209}Bi+^{136}Xe systems an average charge diffusion coefficient of approximately 0.5×10^{22} s^{-1} is determined in the sticking limit.

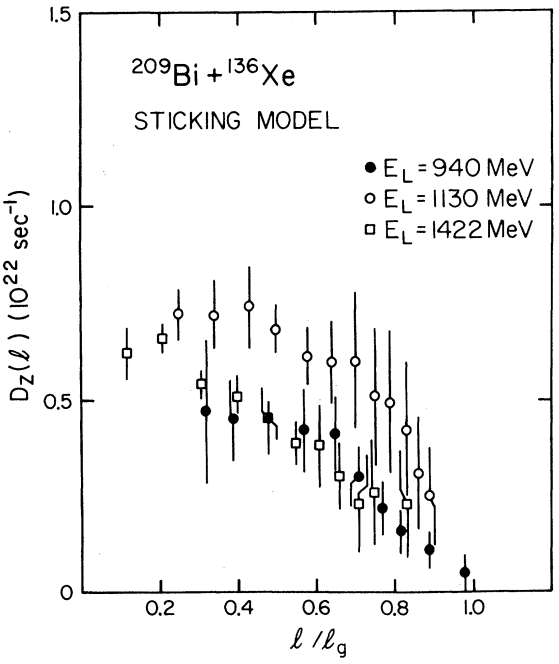

FIG. 6. The average charge diffusion coefficient D_Z is plotted versus the initial relative angular momentum l/l_g for the ^{209}Bi+ ^{136}Xe reaction. The data correspond to an interaction time in the "sticking" limit.

IV. INTERPRETATION OF THE CORRELATION BETWEEN $\ln\sigma_Z^2$ and E/l_g

All results presented in Sec. III are used below to interpret the correlation shown in Fig. 1 between the variance of the element distribution σ_Z^2 and the ratio E/l_g, where E is the final total kinetic energy and l_g is the grazing angular momentum. As illustrated in Sec. III C, the interaction time t_{int} is characterized by an exponential decrease with increasing angular momentum. In a representation of t_{int} versus the initial relative angular momentum l/l_g, the exponential relationship is found to be independent of the bombarding energy. It is this result of the phenomenological description of a strongly damped reaction that establishes the functional dependence of the variance of the Z distribution on impact parameter. Once the l-dependent parametrization of the nuclear interaction time [Eq. (3.14)] is incorporated into Eq. (3.1), the logarithm of σ_Z^2 becomes a linear function of l/l_g

$$\ln\sigma_Z^2=\ln(2D_Z a)-b(l/l_g)\ . \tag{4.1}$$

In obtaining this expression, the charge diffusion coefficient D_Z is assumed to remain constant for all impact parameters. This assumption is qualitatively justified in Sec. III D, where it is shown that

D_Z is constant except for a region of l values near the grazing angular momentum. It should be emphasized however, that even if the charge diffusion coefficient is assumed to increase linearly from 10^{21} to 10^{22} s^{-1}, the dependence of $\ln\sigma_Z^2$ on l/l_g is still well approximated by a linear function.

Experimental results for the logarithm of σ_Z^2 values are plotted in Fig. 7 as a function of l/l_g for various ^{56}Fe, ^{84}Kr, and ^{136}Xe induced reaction (Refs. 1, 3, 7, 8, 15, and 17) for which the fusion cross section and the differential cross section as a function of negative Q value are known. Under the assumption of a sharp cutoff model ($\delta=0$), the mean intitial angular momentum is extracted from the measured data as described in Sec. III B. As can be seen, there is a nearly linear relationship between $\ln\sigma_Z^2$ and l/l_g which is predicted from Eq. (4.1). All the element distributions develop from a δ function near $l=l_g$ where projectile and target nuclei can only be Coulomb excited. The results in Fig. 7 show that not only the offset but also the slope of the linear function is nearly system independent, especially if one considers the error bars given for two values of the ^{209}Bi+^{136}Xe reaction at $E_L=1130$ MeV. The observed relationship indicates that for each heavy-ion system the variance of the element distribution is governed by the initial relative angular momentum l/l_g.

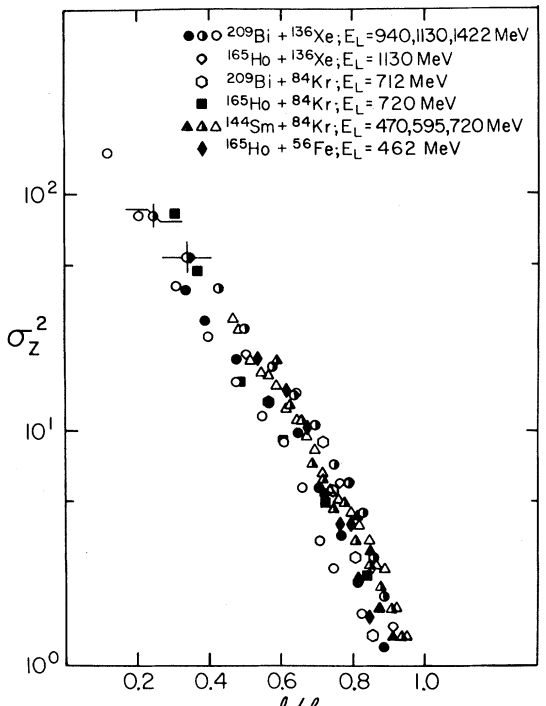

FIG. 7. The variance of the element distribution σ_Z^2 is plotted as a function of the initial relative angular momentum l/l_g for various projectile-target systems (Refs. 1, 3, 7, 8, 15, and 17). The initial angular momentum l has been inferred from the final total kinetic energy. Typical error bars are shown for two values of the ^{209}Bi+^{136}Xe reaction at $E_L=1130$ MeV.

There is a close similarity between the model-dependent correlation of Fig. 7 and the model-independent correlation shown in Fig. 1. The abscissa of Fig. 7 may be transformed into the abscissa of Fig. 1 by making use of the nearly linear relationship between the final total kinetic energy $\langle E\rangle$ and the initial angular momentum $\langle l\rangle$ discusses in Sec. III B. Replacement of l/l_g in Fig. 7 by E/l_g gives the empirical correlation between experimental observables shown in Fig. 1. As discussed in Sec. II, plots of the quantity $\ln\sigma_Z^2$ exhibit a linear dependence on E/l_g for some sixteen different heavy-ion systems. The logarithmic lines are observed to have nearly equal slopes adding evidence to the general relationship shown in Fig. 7. However, in Fig. 1 the data for each individual system are displaced along the E/l_g axis. Each system intercepts the abscissa approximately at E_0/l_g (Fig. 2) which is not unexpected due to the fact that $\ln\sigma_Z^2$ is close to zero for grazing collisions. Therefore, each total kinetic energy loss ($\equiv Q\langle 0$) can be related to a certain width of the element distribution. It is striking to observe that there is a common correlation between $\ln\sigma_Z^2$ and E/l_g applying to such different systems as ^{238}U+^{238}U (Ref. 10) and ^{165}Ho+^{56}Fe (Ref. 17), and a bombarding-energy range from 1.9 to 5.3 MeV/nucleon above the Coulomb barrier in the case of the ^{209}Bi+^{136}Xe reaction.[3,7,8] The unique correlation obtained suggests an extrapolation of the dependence of the variance σ_Z^2 on E/l_g into the region of higher incident energies. Even the broadest element distributions expected in a strongly damped collision can be predicted, because the minimum final total kinetic energy is well reproduced by a formula[18,25] derived from the study of fissioning nuclei. The present correlation of the experimental data is a more general representation of the data than the previous correlation of $E_{\rm loss}$ vs σ_Z^2 which emphasizes the properties of the projectile-target combination. Hopefully, the correlation of σ_Z^2 with l/l_g will give new insights to our understanding of dissipative phenomena.

Some remarks are in order concerning heavy-ion reactions at bombarding energies very close to the Coulomb barrier, $E_0/V_C(R_{\rm int})=1.01-1.20$,[23]

which show a different behavior of $\ln\sigma_Z^2$ vs E/l_g. For final total kinetic energies between the incident energy E_0 and the Coulomb energy of touching spherical nuclei $V_C(R_{\rm int})$, the $\ln\sigma_Z^2$ data follow the general systematics presented here. However, for smaller final total kinetic energies the variance of the Z distribution increases more slowly than predicted from systematics at higher bombarding energies. The discontinuity in the low-energy region is probably not related to a drastic change in the nuclear interaction time which is well described by only one exponential function. Rather, for bombarding energies close to the barrier, the relation between $\langle E\rangle$ and $\langle l\rangle$ is expected to deviate from the linear function relatively well defined for reactions at higher bombarding energies.

V. CONCLUSIONS

The observed correlation between the variance of the element distribution σ_Z^2 and the ratio E/l_g of the final total kinetic energy E to the grazing angular momentum l_g has been investigated on the basis of a phenomenological model[4–6] combined with a diffusion model.[9] In the framework of the phenomenological model the experimental energy spectrum $d\sigma/d(-Q)$ and the mean values $\langle\theta(E)\rangle$ of the angular distribution $d^2\sigma/dE\,d\Omega_{\rm c.m.}$ are parametrized in terms of the initial angular momentum l and the nuclear interaction time $t_{\rm int}$. Numerical values have been deduced from a fit to the particular reaction ^{209}Bi+^{136}Xe at $E_L=940$, 1130, and 1422 MeV, serving as a representative example of damped reactions. In agreement with other heavy-ion reactions the deduced interaction time for this system increases exponentially with decreasing initial relative angular momentum l/l_g with a rate that is nearly independent of the bombarding energy. This functional form inserted into the relation $\sigma_Z^2=2D_Zt_{\rm int}$ of the diffusion model,[9] together with the assumption of a nearly constant average charge diffusion coefficient D_Z, leads to a semiempirical expression that has a linear dependence of the logarithm of σ_Z^2 on the initial relative angular momentum l/l_g. A semilogarithmic plot of the experimental values of σ_Z^2 as a function of the model-dependent values of l/l_g confirms the latter semiempirical formula. Completely unexpected, however, is the result that the slope of this function is independent of the heavy-ion system as shown in Fig. 7. It is apparent from this diagram that the width of the final element distribution is determined by the initial relative angular momentum l/l_g or the corresponding impact parameter ratio b/b_g.

In conjunction with the deduced nearly linear relationship between the final total kinetic energy $\langle E\rangle$ and the initial angular momentum $\langle l\rangle$, the new representation of $\ln\sigma_Z^2$ as a function of E/l_g, which depends only on measured observables, follows immediately. The final element distribution develops from a δ function near $E=E_0$ and reaches its largest variance for a minimum total kinetic energy approximated by a slightly modified version[18] of the well known general fission systematics of Viola.[25] The most interesting feature of this presentation is the fact that the σ_Z^2 data lie on nearly parallel lines, when plotted versus E/l_g, for different projectile-target combinations and bombarding energies that are well above the Coulomb barrier. This result shows a close similarity to the entrance channel effect of the model-dependent correlation between $\ln\sigma_Z^2$ and l/l_g.

ACKNOWLEDGMENTS

This work was supported by the U. S. Department of Energy. Helpful discussions with W. U. Schröder are gratefully acknowledged.

---

*Permanent address: GSI, D-6100 Darmstadt, Germany.

[1]J. R. Huizenga, J. R. Birkelund, W. U. Schröder. K. L. Wolf, and V. E. Viola, Jr., Phys. Rev. Lett. 37, 885 (1976).

[2]T. Tanabe, R. Bock, M. Dakowski. A. Gobbi, H. Sann, H. Stelzer, U. Lynen, A. Olmi, and D. Pelte, Nucl. Phys. A342, 194 (1980).

[3]H. J. Wollersheim, W. W. Wilcke, J. R. Birkelund, J. R. Huizenga, W. U. Schröder, H. Freiesleben, and D. Hilscher, Phys. Rev. C. (in press).

[4]J. R. Huizenga, Nukleonika 20, 291 (1975).

[5]J. P. Bondorf, J. R. Huizenga, M. I. Sobel, and D. Sperber, Phys. Rev. C 11, 1265 (1975).

[6]W. U. Schröder, J. R. Birkelund, J. R. Huizenga, K. L. Wolf, and V. E. Viola, Jr., Phys. Rev. C 16, 623 (1977).

[7]W. U. Schröder, J. R. Birkelund, J. R. Huizenga, K. L.

Wolf, and V. E. Viola, Jr., Phys. Rep. 45C, 301 (1978).

[8]W. W. Wilcke, J. R. Birkelund, A. D. Hoover, J. R. Huizenga, W. U. Schröder, V. E. Viola, Jr., K. L. Wolf, and A. C. Mignerey, Phys. Rev. C 22, 123 (1980).

[9]W. Nörenberg, Phys. Lett. 52B, 289 (1974).

[10]H. Freiesleben, K. D. Hildenbrand, F. Pühlhofer, W. F. W. Schneider, R. Bock, D. v. Harrach, and H. J. Specht, Z. Phys. A 292, 171 (1979).

[11]U. Lynen, Y. Civelekoglu, A. Olmi, H. Sann, D. Pelte, R. Bock, A. Gobbi, and H. Stelzer, GSI Jahresbericht, 1977, GSI-J-1-78, p.55.

[12]H. Sann, A. Olmi, Y. Civelekoglu, D. Pelte, U. Lynen, H. Stelzer, A. Gobbi, Y. Eyal, W. Kohl, R. Renfordt, I. Rode, G. Rudolf, D. Schwalm, and R. Bock, Proceedings of the Conference on Heavy Ion Collisions, Fall Creek Falls State Park, Pikeville, Tennessee, 1977, CONF-770602, p.281.

[13]E. C. Wu, K. D. Hildenbrand, H. Freiesleben, A. Gobbi, U. Lynen, A. Olmi and H. Sann, GSI Jahresbericht, 1979, GSI 80-3, p.14.

[14]G. Rudolf, A. Gobbi, H. Stelzer, U. Lynen, A. Olmi, H. Sann, R. G. Stokstad, and D. Pelte, Nucl. Phys. A330, 243 (1979); M. Dakowski, P. Doll, A. Gobbi, G. Rudolf, H. Sann, R. Bock, U. Lynen, and A. Olmi, Phys. Lett. 90B, 379 (1980).

[15]A. C. Mignerey (unpublished).

[16]M. P. Webb, dissertation, University of Washington, Seattle, 1977.

[17]A. D. Hoover, J. R. Birkelund, D. Hilscher, W. U. Schröder, W. W. Wilcke, J. R. Huizenga, H. Breuer, A. C. Mignerey, V. E. Viola, Jr., and K. L. Wolf, Phys. Rev. C 25, 256 (1982).

[18]W. W. Wilcke, J. R. Birkelund, H. J. Wollersheim, A. D. Hoover, J. R. Huizenga, W. U. Schröder, and L. E. Tubbs, At. Data Nucl. Data Tables 25, No. 5 (1980); 25, No. 6 (1980).

[19]M. Dakowski, P. Doll, A. Gobbi, U. Lynen, A. Olmi, G. Rudolf, H. Sann, and R. Bock, Proceedings of the International Symposium on Continuous Spectra of Heavy Ion Reactions, San Antonio, Texas, 1979, ISSN:0250-4375, p.1.

[20]C. Riedel, G. Wolschin, and W. Nörenberg, Z. Phys. A 290, 47 (1979).

[21]J. R. Huizenga, W. U. Schröder, J. R. Birkelund, and W. W. Wilcke, Proceedings of the Conference of Heavy Ion Collisions, Fall Creek Falls State Park, Pikeville, Tennessee, 1977, CONF-770602, p.179.

[22]W. U. Schröder and J. R. Huizenga, Annu. Rev. Nucl. Sci. 27, 465 (1977).

[23]W. E. Frahn, Nucl. Phys. A302, 267 (1978).

[24]A. Olmi, H. Sann, D. Pelte, Y. Eyal, A, Gobbi, W. Kohl, U. Lynen, G. Rudolf, H. Stelzer, and R. Bock, Phys. Rev. Lett. 41, 688 (1978).

[25]V. E. Viola, Jr., Nucl. Data Sect. A1, 391 (1966).

[26]G. Wolschin, Nukleonika 22, 1165 (1977).

[27]G. Wolschin and W. Nörenberg, Z. Phys. A 284, 209 (1978).

[28]G. Wolschin and W. Nörenberg, Phys. Rev. Lett. 41, 691 (1978).

[29]K. E. Rehm. P. Sperr, K. Hartel, P. Kienle, H. J. Körner, R. E. Segel, and W. Wagner, Lecture Notes in Physics, 117, 127 (1980); Phys. Lett. (to be published).